

# The correlation functions of certain random antiferromagnetic spin-1/2 critical chains

João C. Getelina<sup>1,2</sup> and José A. Hoyos<sup>1</sup>

<sup>1</sup>*Instituto de Física de São Carlos, Universidade de São Paulo, CP 369, 13560-970, São Carlos, SP, Brazil*

<sup>2</sup>*Department of Physics, Missouri University of Science and Technology, Rolla, MO 65409, USA*

(Dated: January 29, 2020)

We study the spin-spin correlations in two distinct random critical XX spin-1/2 chain models via exact diagonalization. For the well-known case of uncorrelated random coupling constants, we study the non-universal numerical prefactors and relate them to the corresponding Lyapunov exponent of the underlying single-parameter scaling theory. We have also obtained the functional form of the correct scaling variables important for describing even the strongest finite-size effects. Finally, with respect to the distribution of the correlations, we have numerically determined that they converge to a universal (disorder-independent) non-trivial and narrow distribution when properly rescaled by the spin-spin separation distance in units of the Lyapunov exponent. With respect to the less known case of correlated coupling constants, we have determined the corresponding exponents and shown that both typical and mean correlations functions decay algebraically with the distance. While the exponents of the transverse typical and mean correlations are nearly equal, implying a narrow distribution of transverse correlations, the longitudinal typical and mean correlations critical exponents are quite distinct implying much broader distributions. Further comparisons between these models are given.

## I. INTRODUCTION

Random quantum spin chains have proved to be a fruitful platform for developing new methodologies and fundamental concepts in condensed matter physics. One of the most successful methods developed so far is the so-called strong-disorder renormalization-group (SDRG) method [1–3], which has been applied to a plethora of random systems (see Refs. 4 and 5 for reviews). Inherently linked to it is the concept of infinite-randomness fixed points [6, 7]. These are critical points in which the statistical fluctuations of local quantities, surprisingly, increase without limits along the renormalization-group flow yielding to an exotic type of activated dynamical scaling. Equally important, due to the unbounded increase of the statistical fluctuations, the SDRG method is believed to exactly capture the universal properties of these fixed points. Finally, it is noteworthy that these fixed points control the phase transitions and critical phases of many quantum, classical and non-equilibrium disordered systems (see Ref. 8 for a review).

In this context, the random antiferromagnetic quantum spin-1/2 chain is a paradigmatic model which for many years has been stimulating theoretical [1, 2, 7, 9–16] and experimental [17–20] studies. For a large range of anisotropies, it is a critical system governed by an infinite-randomness fixed point amenable to many analytical predictions of the SDRG method. A striking one is that the average value spin-spin correlations decays algebraically with the distance  $\sim r^{-\eta_\alpha}$  with universal (disorder-independent) isotropic exponent  $\eta_x = \eta_z = 2$ , while the typical value decays stretched exponentially fast  $\sim e^{-\sqrt{r}}$  [7].

Nonetheless, this knowledge is far from satisfactory when compared to the clean chain. Not only the exponents of the leading and subleading terms are known, but also the corresponding numerical prefactors [21–32]. It is the purpose of this work to shorten the knowledge gap between clean and disordered systems by studying non-universal (disorder-dependent) details of the spin-spin correlation functions, such as the numerical prefactors and scaling variables.

Recently, it was discovered that the paradigmatic random

antiferromagnetic quantum spin-1/2 chain can also be governed by a line of finite-disorder fixed points when a certain type of correlations are present in the random coupling constants [15, 33, 34]. This is an exciting result not only because it allows us studying new physical phenomena in a simple and well-known model, but also because the correlations among the disorder variables are the same present in a class of polymers [35–37]. However, unlike the uncorrelated disorder model, much less is known about its average correlation function. Nothing about the typical correlations are known. For this reason, it is also the purpose of this work to study the corresponding critical exponents.

In Sec. II, we define the models studied, review further relevant results for our purposes, and provide the methodology of our study. In Secs. III and IV we report our results on the correlation functions of the uncorrelated and correlated disordered spin chains, respectively. Finally, we provide further discussions and concluding remarks to Sec. V.

## II. MODELS, KNOWN RESULTS AND METHODS

In this section we define the studied models, review key known results in the literature about the spin-spin correlation functions, and explain our methods.

### II.1. Models

The Hamiltonian of the random XXZ spin-1/2 chain is

$$H = \sum_{i=1}^L J_i (S_i^x S_{i+1}^x + S_i^y S_{i+1}^y + \Delta S_i^z S_{i+1}^z), \quad (1)$$

where  $S_i^\alpha$  are spin-1/2 operators,  $J_i$  are the random coupling constants, and  $\Delta$  is the anisotropy parameter. We consider chains of even size  $L$  with periodic boundary conditions  $S_{i+L}^\alpha = S_i^\alpha$ . The coupling constants  $J_i$  are realizations of a ran-

arXiv:1910.00631v2 [cond-mat.dis-nn] 28 Jan 2020

dom variable drawn from the probability distribution

$$P(J) = \begin{cases} \frac{1}{D} J^{D-1}, & \text{if } 0 < J < 1 \\ 0, & \text{otherwise.} \end{cases} \quad (2)$$

Here, the disorder strength is parameterized by  $D \geq 0$ , with  $D = 0$  representing the uniform (clean) system and  $D \rightarrow \infty$  representing an infinitely disordered system. In addition, we consider the cases of (i) uncorrelated couplings  $\overline{J_i J_k} = \overline{J_i} \times \overline{J_k}$  and (ii) perfectly and locally correlated couplings such that the coupling sequence is  $\{J_1 J_1 J_2 J_2 \dots J_{\frac{L}{2}} J_{\frac{L}{2}}\}$ , with  $\overline{J_i J_k} = \overline{J_i} \times \overline{J_k}$ .

Finally, in this work we will consider only the  $\Delta = 0$  case.

## II.2. Some known results for the case of uncorrelated couplings

For uncorrelated random couplings, the SDRG method predicts that the low-energy critical physics of (1) is governed by an infinite-randomness critical fixed point for  $-\frac{1}{2} < \Delta \leq 1$  [7, 9]. It is universal in the sense that the corresponding singular behavior does not depend on  $P(J)$  provided that  $P(J < 0) = 0$  and it is not excessively singular at  $J = 0$  [7]. In addition, the method predicts that a good approximation of the corresponding ground state is the random-singlet state (as depicted in Fig. 1) from which much information about the physics can be obtained.

The first one is that spin pairs become locked into SU(2)-symmetric singlet states, and thus, the bare SO(2) symmetry of (1) is enhanced to SU(2). As a consequence, the universal properties of the system become SU(2) isotropic.<sup>1</sup>

Another useful information is related to the distribution of the singlet lengths which decays as  $\frac{2}{3}r^{-2}$  [12] for lengths  $1 \ll r \ll L$ . Since those singlets are strongly correlated, they dominate the (arithmetic average) mean spin-spin correlation function. Thus,

$$\overline{C^{\alpha\alpha}(r)} \equiv \overline{\langle S_i^\alpha S_{i+r}^\alpha \rangle} = \frac{(-1)^r}{12r^\eta} \times \begin{cases} c_{o,\alpha}, & \text{for } r \text{ odd} \\ c_{e,\alpha}, & \text{for } r \text{ even} \end{cases}, \quad (3)$$

with universal and isotropic exponent  $\eta = 2$ , and non-universal and anisotropic multiplicative constants  $c_{o,e,\alpha} \geq 0$ .<sup>2</sup> Surprisingly, it was conjectured [12] that  $c_{o,\alpha} - c_{e,\alpha} = 1$  is universal for  $\alpha$  being a symmetry axis, i.e., for  $\alpha = z$ , and for any  $\alpha$  when  $\Delta = 1$ . (Here,  $\langle \dots \rangle$  and  $\overline{\dots}$  denote the quantum and the disorder averages, respectively.)

The universality of the exponent  $\eta$  was disputed some years ago [41], but there is now a consensus that this is an exact result [10, 42–44]. Evidently, numerical confirmations of the constants  $c_{e,o,\alpha}$  are much more difficult [12, 34].

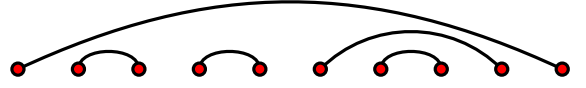


FIG. 1. Schematic of the random-singlet state, which gives the approximate ground state of the Hamiltonian (1) for  $-\frac{1}{2} < \Delta \leq 1$ , according to the strong-disorder renormalization group method.

We note that logarithmic corrections to (3) have been reported in numerical studies for the free-fermion case  $\Delta = 0$  [43] in which

$$\overline{C^{\alpha\alpha}} \sim (r^\eta \ln r)^{-1}, \quad (4)$$

and for the Heisenberg case  $\Delta = 1$  [16] in which<sup>3</sup>

$$\overline{C^{\alpha\alpha}} \sim r^{-\eta} \sqrt{\ln r / r_0}. \quad (5)$$

In contrast, the (geometric average) typical spin-spin correlation function behaves completely different since the spin pairs are weakly coupled in the great majority, as depicted in Fig. 1. It was then conjectured [7] that the quantity  $r^{-\psi} \ln |\langle S_i^\alpha S_{i+r}^\alpha \rangle|$  converges to a distance-independent distribution. Therefore,

$$C_{\text{typ}}^{\alpha\alpha}(r) \equiv \exp \overline{\ln |\langle S_i^\alpha S_{i+r}^\alpha \rangle|} \sim \exp(-\text{const} \times r^\psi), \quad (6)$$

with universal and isotropic tunneling exponent  $\psi = \frac{1}{2}$ . This result was confirmed in Ref. [42] but its dependence with the disorder strength (encoded in the constant prefactor) remains unknown.

## II.3. Some known results for the case of correlated couplings

In contrast, for the case of locally correlated couplings (the sequence of couplings being  $\{J_1, J_1, J_2, J_2, \dots, J_{\frac{L}{2}}, J_{\frac{L}{2}}\}$ ) and anisotropy parameter  $\Delta = 0$ , the physics is quite different [15, 33, 34].

For weak disorder  $D < D_c \approx 0.3$ , the critical properties are those of the clean system, i.e., weak disorder is an irrelevant perturbation. Hence, the mean and typical values of the correlation functions are approximately equal, and the corresponding exponents are those of the clean system, i.e.,  $C^{\alpha\alpha} \approx C_{\text{clean}}^{\alpha\alpha} \sim r^{-\eta_\alpha}$ , with  $\eta_x = \frac{1}{2}$  and  $\eta_z = 2$ .

For  $D > D_c$ , a line of finite-disorder fixed points is tuned and thus the critical exponents vary continuously with the disorder strength [33]. However, in contrast with the infinite-randomness case, we only know that the longitudinal mean correlations decays algebraically with apparently disorder-independent exponent  $\eta_z \approx 2$  [34].

We recall that the effects of long-range correlated disorder in closely related systems have been studied in Refs. 45 and

<sup>1</sup> This phenomenon of symmetry enhancing is known to be general in random antiferromagnetic SO( $N$ ) spin chains exhibiting SU( $N$ ) symmetric singular properties [38–40].

<sup>2</sup> For  $\Delta = 0$ , the longitudinal correlation between spins in the same sublattice vanishes, and thus,  $c_{e,z} = 0$  [21].

<sup>3</sup> While the SDRG method have been believed to deliver asymptotic exact results for the XXZ spin chain (1), these numerical results cast some doubts on this belief. As shown latter, our results do not exhibit any logarithmic correction.

46. It was shown that disorder effects are actually enhanced, i.e., the critical theory is of infinite-randomness type accompanied with offcritical enhanced Griffiths singularities. We stress that our correlated disorder has the quite opposite effect [33].

#### II.4. Methods and further motivations

One of our main goals is to study the non-universal numerical prefactors of the correlation functions. As there is no analytical theory capable of dealing with the clean and random systems on the same footing, we then resort to exact diagonalization of large systems. This is possible only for the  $\Delta = 0$  case via the mapping of the Hamiltonian (1) into free spinless fermions [21].

Nonetheless, this is not as simple as it looks. Due to the singularities of strongly disordered systems (namely, large dynamical exponent), we had to use quadruple precision (32 decimal places) in the numerical diagonalization process.

Moreover, regarding the choice of  $\Delta = 0$ , even though it represents a “non-interacting” system, notice it captures the universal infinite-randomness quantum critical properties (as predicted by the SDRG method) of the entire  $-\frac{1}{2} < \Delta < 1$  line, i.e., interactions are RG irrelevant in this range [7]. For the case of correlated couplings, studying the  $\Delta = 0$  case is imperative since the finite-disorder character can only be explored for  $\Delta = 0$  [34].

Finally, given that the SDRG method is believed to provide exact results concerning the critical singularities of the model (1), it is desirable to investigate large system sizes in order to check the logarithmic corrections mentioned in Eqs. (4) and (5). The motivation for searching them is justified in the early works of homogeneous XXZ spin-1/2 chains [25–27, 29–31, 47], and also in a recent work of the random XXZ model at  $\Delta = -\frac{1}{2}$  [13]. We anticipate that our results are in agreement with (3).

### III. SPIN-SPIN CORRELATIONS FOR THE UNCORRELATED COUPLING CONSTANTS MODEL

We show in this section our results on the (arithmetic average) mean and (geometric average) typical spin-spin correlation functions in the ground state of (1) for  $\Delta = 0$  and for uncorrelated disordered coupling constants. We have used quadruple precision (32 decimal places) in order to ensure numerical stability.

#### III.1. The mean value of the critical correlation function

We start our study with the mean correlation function. All data here presented were averaged over  $N = 10^6$  distinct disorder realizations, except for those cases of system size  $L = 1600$  in which  $N = 10^5$ .

##### III.1.1. Longitudinal correlations

In Fig. 2, we show  $\overline{C^{zz}}$  for fixed system size  $L = 800$  and various disorder strengths  $D$  in panel (a), and fixed  $D = 2.0$  and various system sizes  $L$  in panel (b). The algebraic decay  $\overline{C^{zz}} \sim Ar^{-2}$  is identical in both clean and disordered case. The difference is in the numerical prefactor:  $A = \pi^{-2}$  in the clean case [21], and is conjectured to be  $1/12$  in the disordered case [12]. As we are interested in the long-distance behavior  $r \gg \xi_D$  (but not restricted to  $r \ll L$ ), with  $\xi_D$  being a clean-disorder crossover length yet to be defined, we then assume that the longitudinal correlation function is

$$\overline{C^{zz}}(r) = -\frac{1}{12}\chi_z(D, r) \left( \ell f_z \left( \frac{r}{L} \right) \right)^{-\eta}, \quad (7)$$

where  $\eta = 2$ ,

$$\ell = \frac{L}{\pi} \sin \left( \frac{\pi r}{L} \right), \quad (8)$$

is the chord length,<sup>4</sup>

$$f_\alpha(x) = 1 + \sum_{n=1}^{\infty} a_{2n,\alpha} \sin^{2n}(\pi x), \quad (9)$$

(with  $\alpha = x$  or  $z$ ) and  $\chi_z$  is a crossover function which assumes the value  $12\pi^{-2}$  in the small separation limit ( $r \ll \xi_D$ ) and converges to 1 otherwise. From Fig. 2(a), it clearly converges to 1 non-monotonically with respect to  $D$  and, from Fig. 2(b), the convergence happens only after long separations. This non-monotonic behavior can be also seen in Fig. 2(c) where the mean correlation for nearest neighbors,  $r = 1$ , is plotted as a function of  $D$  for  $L = 800$ . Initially it increases (as expected according to the random singlet picture) but then diminishes for larger  $D$ . Evidently, this non-monotonic behavior is related to the total spin conservation in the  $z$  direction. In other words,  $\chi_z$  is a non-trivial crossover function and will not be studied here.

In the large separation regime  $r \gg \xi_D$ , the main dependence of  $\overline{C^{zz}}$  on  $r$  comes as  $\ell f_z \left( \frac{r}{L} \right)$ . Simply, it is the most generic function consistent with the periodic boundary conditions:  $C(r+L) = C(r)$  and  $C(L-r) = C(r)$ ; with  $f_z$  being simply a correction to the chord length  $\ell$ : the true scaling variable in the clean case  $C_{\text{clean}}^{zz} = (\pi\ell)^{-2}$ .<sup>5</sup>

Throughout this work, we assume that the coefficients  $a_{2n,\alpha}$  are disorder-independent. There is no reason why this should be the case. Our assumption, however, is compatible with our numerical data. Nonetheless, due to statistical fluctuations and the lack of knowledge on  $\chi_\alpha$ , we cannot exclude that  $a_{2n,\alpha}$  are indeed disorder dependent.

In order to obtain the correction to the chord length, we appropriately replot our data in Fig. 3. In panel (a), we consider only the largest and strongest disordered chains in order

<sup>4</sup> If the spins were arranged in a circle of perimeter  $L$ , then the chord length  $\ell$  is the Euclidean distance between them.

<sup>5</sup> Corrections to the chord length were reported in the entanglement entropy as well [48].

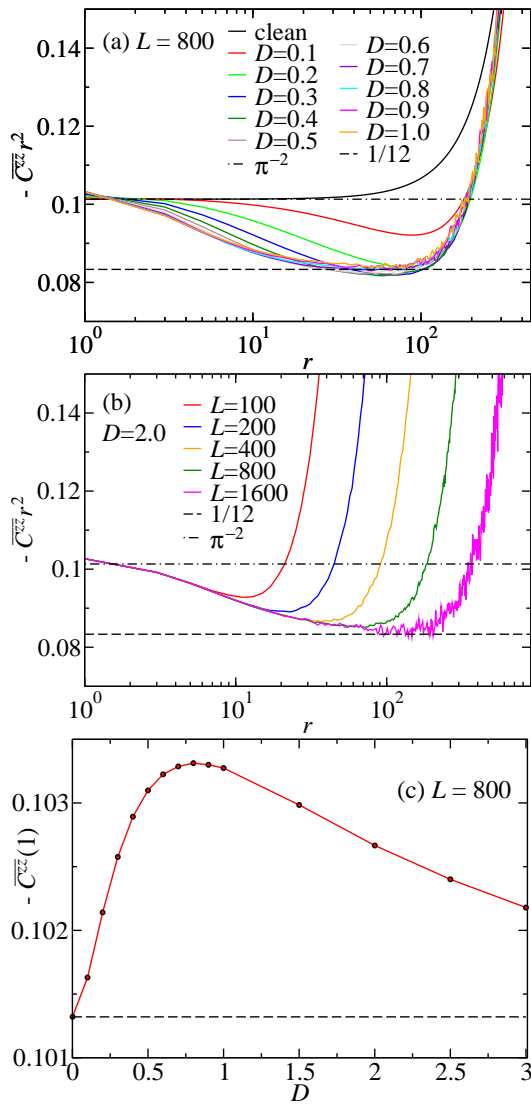


FIG. 2. The mean longitudinal correlation function  $\overline{C^{zz}}(r)$  for various chain sizes  $L$  and disorder strengths as a function of the separation  $r$  in panels (a) and (b), and  $\overline{C^{zz}}(r=1)$  for various  $D$  and  $L=800$  in panel (c).

to minimize the effects of the crossover function  $\chi_z$ , i.e., we have chosen only systems in which  $\chi_z$  seems to be very close to 1 for a large range of separations  $r$ . All data collapse satisfactorily. Tiny deviations are present which, in principle, are accounted by  $\chi_z$ . From the collapsed data, we then extract the values of the coefficients  $a_{2n,z}$ . Best fits using further corrections (up to  $a_{8,z}$ ) do not improve the reduced weighted error sum  $\bar{\chi}^2$ . Finally, changing the fitting values of  $a_{2n,z}$  by 10% does not change appreciably the value of  $\bar{\chi}^2$ , we then estimate that 10% is the accuracy of our estimates of  $a_{2n,z}$ .

In Figs. 3(b) and (c), we plot the square root of the ratio between  $-12\overline{C^{zz}}$  and  $(\ell f_z(\frac{r}{L}))^{-1}$  which should approach 1 provided that  $f_z$  is disorder independent. In panel (b), disorder strength is fixed while  $L$  is increased. Larger the system size  $L$ , better the data is described by the scaling variable  $\ell f_z(\frac{r}{L})$ . Deviations for smaller  $L$  are due to the crossover function  $\chi_z$ . In panel (c), the system size is fixed while  $D$  is changed. No-

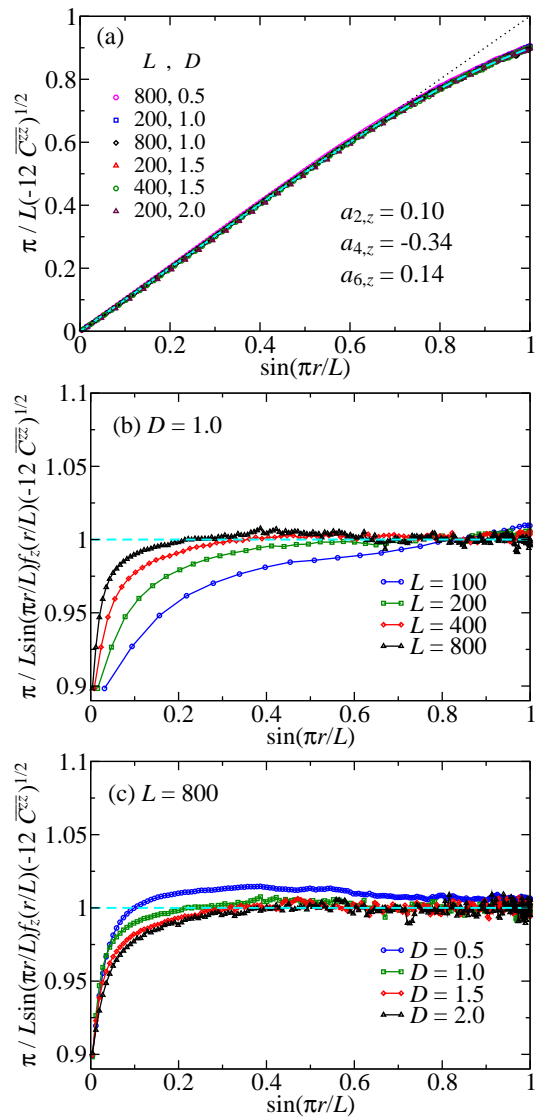


FIG. 3. The mean longitudinal correlation  $\overline{C^{zz}}$  as a function of  $\sin(\pi r/L)$  re-scaled in many different ways in order to obtain the correction in Eq. (9) (see text). The dashed line in panel (a) corresponds to our best fit:  $a_{2,z} = 0.135$ ,  $a_{4,z} = -0.414$  and  $a_{6,z} = 0.179$ . The dotted line is simply the identity function.

tice the little dependence on  $D$  (for large  $L$  and the disorder strengths considered). Notice furthermore the non-monotonic behavior of  $\chi_z$  with  $D$ . The convergence to the unity is faster for intermediate disorder  $D \approx 1.0$ .

### III.1.2. Transverse correlations

The study of the mean transverse correlation function  $\overline{C^{xx}}(r)$  is much more involving since (i) it is more numerically demanding,<sup>6</sup> (ii) there is no knowledge about its numerical

<sup>6</sup> It requires the computation of a large determinant [21] which makes it more prone to numerical round-off errors.



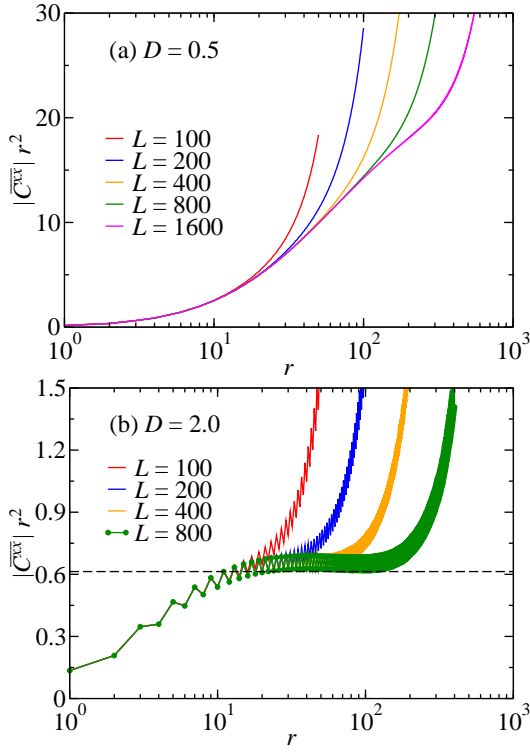


FIG. 4. The mean transverse correlation function  $|\overline{C^{xx}}(r)|$  for various chain sizes  $L$  and disorder strengths (a)  $D = 0.5$  and (b)  $D = 2.0$ .

prefactor, and, as shown in Ref. 10, (iii) the clean-disorder crossover length can be so large that even hinders the clear identification of the correct algebraic decay exponent  $\eta = 2$  (see Fig. 4). Moreover and interestingly, as clearly seen in Fig. 4(b), this numerical prefactor is different from odd and even separations  $r$ .<sup>7</sup>

As for the longitudinal correlations (7), the natural choice for the mean transverse correlation function is

$$\overline{C^{xx}}(r) = (-1)^r c_{D,r} \chi_x(D, r) \left( \ell f_x \left( \frac{r}{L} \right) \right)^{-\eta}, \quad (10)$$

where  $\eta = 2$ , and  $f_x$  is analogous to  $f_z$  in Eq. 9. Likewise, the crossover function  $\chi_x$  is expected to be analogous to  $\chi_z$ , and thus, is a non-trivial function which should be proportional to  $\sim r^{3/2}$  in the  $r \ll \xi_D$  regime, and converges to 1 otherwise. Here,  $c_{D,r}$  represents the numerical prefactor which, in the large separation limit, equals to

$$c_{D,r} = \frac{1}{24} (c_{o,D} + c_{e,D} - (-1)^r (c_{o,D} - c_{e,D})), \quad (11)$$

with  $c_{o(e),D}$  being the absolute value of the prefactor corresponding to odd (even) separations (multiplied by 12, for comparison with  $\overline{C^{zz}}$ ).

In order to obtain the chord-length correction  $f_x$ , it is helpful to have some knowledge of the prefactor  $c_{D,r}$ . Naively, one

could obtain its dependence with  $D$  by simply connecting the clean and disordered behaviors, i.e., given that  $C_{\text{clean}}^{xx} = A/\sqrt{r}$  and that  $\overline{C^{xx}} = c_{D,r}/r^2$ , then  $C_{\text{clean}}^{xx} = \overline{C^{xx}}$  at, say, a sharp crossover length  $r = \xi_D$ . Hence,  $c_{D,r} \sim \xi_D^{3/2}$  and thus, we need knowledge on the crossover length.

Using field-theory methods (accurate at the weak-disorder limit  $D \ll 1$ ), it was shown that  $\xi_D \sim 1/\text{var}(J) = D^{-2}(1+D)^2(1+2D)$ . However, while this relation is accurate for small  $D$ , it was numerically found that  $\xi_D \sim D^{-(2.0 \pm 0.2)}$  is much more satisfactory for any  $D$  [10]. Later, it was shown that a single-parameter theory holds at the band center of particle-hole symmetric tight-binding chains [49] [which maps to the Hamiltonian (1)]. The wavefunction is stretched-exponentially localized with the inverse of the Lyapunov exponent (or localization length) being<sup>8</sup>

$$\gamma_D^{-1} = \frac{\pi}{8\text{Var}(\ln J)} = \frac{\pi}{8D^2}. \quad (12)$$

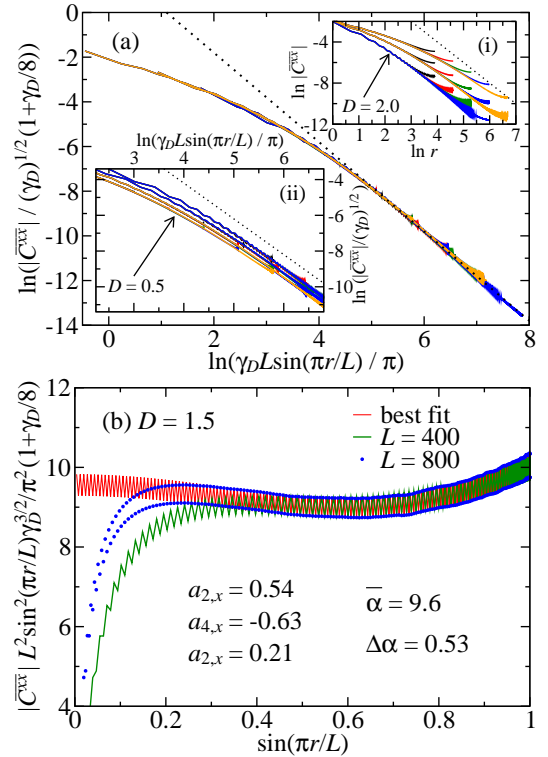


FIG. 5. (a) The mean transverse correlation function  $\overline{C^{xx}}$  as a function of the spin separation  $r$  for various disorder strengths  $D = 0.5$ ,  $D = 1.0$ ,  $D = 1.5$  and  $D = 2.0$  and system sizes  $L = 100$  (black), 200 (red), 400 (green), 800 (blue) and 1600 (orange, and only for  $D = 0.5$  and 1.0). For clarity, the data for  $D = 1.5$  is not shown in inset (i). The dotted lines are  $y \sim x^{-2}$  for comparison. (b) The data is rescaled in order to highlight the correction to the chord length scaling (see text). In addition, the numerical prefactors in (14) can be extracted via a fitting and are  $\bar{\alpha} = 9.6(2)$ ,  $\Delta\alpha_{D=0.5} = 0.018(3)$ ,  $\Delta\alpha_{D=1.0} = 0.18(1)$ ,  $\Delta\alpha_{D=1.5} = 0.53(1)$ , and  $\Delta\alpha_{D=2.0} = 1.06(2)$ .

<sup>7</sup> In the clean case [22], the prefactor  $\approx 0.14709$  and is the same for both even and odd separations.

<sup>8</sup> Comparing the definition of the Lyapunov exponent (12) with the values of the crossover length numerically provided in Ref. 10, we simply find that  $\xi_D \approx 51\gamma_D^{-1} \approx 20D^{-2}$ .

With those arguments in mind, we now try to rescale the  $\overline{C}^{xx}$  [shown in the inset (i) of Fig. 5(a)] appropriately. Given that (i)  $c_{D,r} \sim \gamma_D^{-3/2}$  (naive crossover), that (ii) the natural length scale is  $\gamma_D^{-1}$  and that (iii) the chord length  $\ell$  is weakly corrected, we then rescale the chord length in units of  $\gamma_D^{-1}$  and, therefore,  $\overline{C}^{xx}$  must scale as  $\sim \sqrt{\gamma_D}$ . Somewhat surprisingly, with this naive rescaling [see inset (ii) of Fig. 5(a)] we almost achieve a perfect data collapse. In order to improve the data collapse, we fit the data in the inset (ii) to a power-law function  $A(\gamma_D \ell)^{-2}$ , and find that  $A \propto 1 + 0.125\gamma_D$  in the long distance regime  $\gamma_D \ell \gg 1$ . We then correct our naive scaling to

$$\overline{C}^{xx} \sim \left(1 + \frac{1}{8}\gamma_D\right) \sqrt{\gamma_D} \quad (13)$$

and plot the resulting data in the main panel of Fig. 5(a). The collapse is remarkable even for small separations, suggesting a crossover function  $\chi_x(D, r) \approx \chi_x(\gamma_D r)$  for  $\gamma_D r \gtrsim 1$ . In addition, we find useful to recast the prefactor (11) as

$$c_{D,r} = \left(1 + \frac{1}{8}\gamma_D\right) \gamma_D^{-3/2} \left(\bar{\alpha} - \frac{1}{2}(-1)^r \Delta\alpha_D\right), \quad (14)$$

where  $\bar{\alpha}$  is disorder independent.

In Fig. 5(b), we plot  $Y = \overline{C}^{xx}(\gamma_D \ell)^2 / \left(1 + \frac{1}{8}\gamma_D\right) \sqrt{\gamma_D}$  as a function of  $X = \sin(\pi r/L)$  in order to obtain the values  $a_{2n,x}$ ,  $\bar{\alpha}$  and  $\Delta\alpha_D$ . This is achieved via, according to (10), fitting  $Y = \chi_x(\bar{\alpha} - \frac{1}{2}(-1)^r \Delta\alpha_D) / f_x(X)$  to our data. For clarity, we have shown only the data for  $L = 400$  and  $800$  and  $D = 1.5$ .<sup>9</sup> Clearly, the crossover function  $\chi_x$  is converged to 1 for  $X \gtrsim 0.4$  (our fitting region) and  $L = 800$ . The best fit is shown as a solid red line. Notice that this plot is similar to those in panels (b) and (c) of Fig. 3.

Finally, it is interesting to observe the prefactor difference  $\Delta c_D = c_{o,D} - c_{e,D}$  and mean value  $\bar{c}_D = \frac{1}{2}(c_{o,D} + c_{e,D})$ . Using the relations (11) and (14), together with the values of  $\Delta\alpha_D$  and  $\bar{\alpha}$  listed in the caption of Fig. 5, we find that  $(\Delta c_D, \bar{c}_D) = (0.46, 244)$ ,  $(0.70, 37)$ ,  $(0.80, 14)$ , and  $(0.89, 8)$  for  $D = 0.5, 1.0, 1.5$ , and  $2.0$ , respectively. Notice it is not much different from 1 for all values of  $D$ . As conjectured in Ref. [12], this difference should be equal 1 for correlations along a symmetry axis. The total magnetization in the  $x$  direction is not conserved. However, perhaps due to the emergent symmetry  $SO(2) \rightarrow SU(2)$  character of the random singlet state, violations of this difference are small when compared to the values of the coefficients themselves.

### III.1.3. Mimicking logarithmic corrections

Having characterized the long-distance ( $\gamma_D r \gg 1$ ) behavior of the transverse mean correlation function Eq. (10), we now

<sup>9</sup> We report that the corresponding curves for  $D = 0.5, 1.0$  and  $2.0$  are quite consistent with the collapse in 5(a). The only difference being on the value of  $\Delta\alpha_D$ . For  $D = 0.5$ , the crossover function  $\chi_x$  is evidently larger yielding a smaller fitting region  $X \gtrsim 0.8$ .

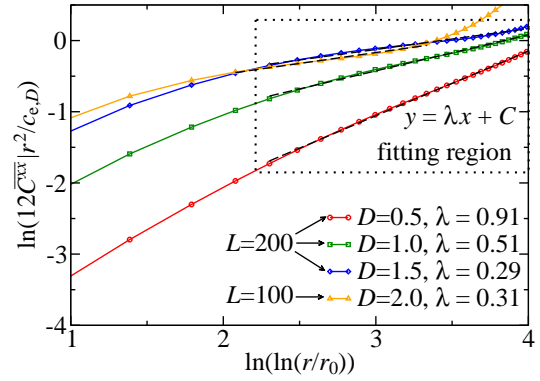


FIG. 6. Mean transverse correlation function  $\overline{C}^{xx}(r)$  plotted according to Eq. (15) for even separations  $r$ , considering various disorder strengths  $D$  and chain sizes  $L$ . The upturn for  $L = 100$  is due to the periodic boundary condition. For comparison, the data is fitted to the function  $y = \lambda x + C$  (dashed lines) within the region compatible with that of Ref. 14.

call attention to their strong finite-size effects when characterizing the random-singlet state in numerical studies via the use of small systems. Interestingly, as can be seen in Fig. 6, the data is compatible with a logarithmic correction to the SDRG prediction of the leading term, i.e., based on small system sizes, one could conclude that

$$\overline{C}^{xx}(r)r^2 \sim \ln^\lambda\left(\frac{r}{r_0}\right). \quad (15)$$

Corrections to the SDRG prediction were reported in the literature over the years, ranging from non-universal critical exponents [41] to logarithmic corrections [14, 43]. Here, we have plotted and fitted our data in the same range compatible with those of Ref. 14 for the Heisenberg random spin chain. The values of the corresponding effective exponent  $\lambda$  are within the range found in that work.

We emphasize that our data show no evidence of logarithmic corrections in the long distance and long chain regime. We also stress that we do not have shown the absence of the logarithmic corrections reported in Ref. 14 (which study the isotropic  $\Delta = 1$  case), we have only showed that the combination of crossover and finite-size effects [as in Eq. (10)] can be interpreted as logarithmic corrections in the case of the XX random spin-1/2 chain. The main culprit being the crossover function  $\chi_x$ .

### III.1.4. Random-singlet correlations

Finally, and just for completeness, we end our study on the mean correlations by focusing only on the main culprits for their behavior: the rare singlet pairs of the random-singlet state (depicted in Fig. 1). Once they are identified (by means of the SDRG decimation procedure [7]), we compute their mean correlations as a function of the separation  $r$  as shown in Fig. 7. The naive expectation based on the clean-disordered crossover is the following. For short distances  $\gamma_D r \ll 1$  (smaller than the crossover length), the correlation

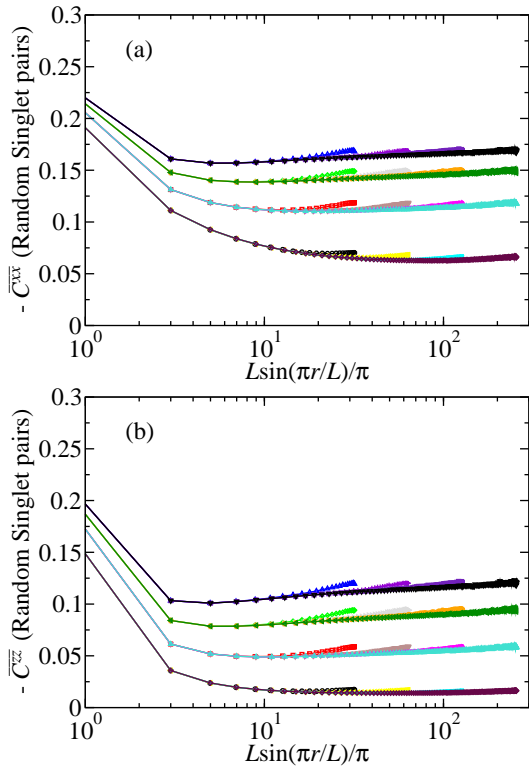


FIG. 7. The mean (a) transverse and (b) longitudinal correlation functions as a function of the chord length  $\ell = \frac{L}{\pi} \sin\left(\frac{\pi r}{L}\right)$  considering only the rare singlets of the random-singlet state obtained via the strong-disorder renormalization-group decimation procedure. The disorder strengths are  $D = 0.5$  (bottommost data sets), 1.0, 1.5 and 2.0 (topmost data sets), and the system sizes are  $L = 100$  (leftmost data sets), 200, 400 and 800 (rightmost data sets).

decays just as in the clean case. For larger distances, on the other hand, the SDRG singlets become a good approximation and thus, their correlations are expected to saturate monotonically and stretched-exponentially fast to a finite value. This expectation is only partially fulfilled as a non-monotonous saturation is observed. In addition, the saturation is much slower than one would expect. (Actually, one could argue that saturation is barely achieved only for the largest and strongest disordered chains.)

Finally, we would like to call attention for the importance of using quadruple precision and having extra care with the numerical instabilities. Using double precision for  $L = 800$  and  $D = 2.0$  yields to data different from those in Fig. 7. Surprisingly, the observed data (not shown here) exhibits a drop in the correlations (due to the inability of capturing the longest and weakest coupled spin pairs) compatible with a logarithmic correction of type (15) with negative exponent of order 1, compatible with that reported in Ref. 43 [see Eq. (4)]. Since these rare singlets dominate the mean correlations, this means that a spurious logarithmic correction can be obtained.

### III.2. Typical correlation function and probability distributions

We now turn our attention to the typical value of the spin-spin correlations [as defined in Eq. (6)]. In this study, we report that our data were averaged over  $N = 10^5$  distinct disorder realizations.

We start by assuming that, in the long-distance regime  $\gamma_D r \gg 1$ , the typical correlations can be well approximated by

$$C_{\text{typ}}^{\alpha\alpha} = (-1)^r c_{\alpha,D} \chi_{\alpha}(D, r) e^{-A_{\alpha} \sqrt{\gamma_D} \ell f_{\alpha}(r/L)}, \quad (16)$$

where  $c_{\alpha,D}$  is a disorder-dependent prefactor,  $\chi_{\alpha}$  represents the crossover function (which  $\chi_{\alpha} \rightarrow 1$  for  $\gamma_D r \gg 1$ ),  $A_{\alpha}$  is a disorder-independent constant,  $\ell$  is the chord length (8),  $\gamma_D$  is the Lyapunov exponent (12), and the correction to the chord length  $f_{\alpha}$  is analogous to those for the average correlations (9). Notice that (16) recovers the SDRG prediction of a stretched exponential decay  $\ln|C_{\text{typ}}^{\alpha\alpha}| \sim -r^{\psi_{\alpha}}$  with universal (disorder-independent) and isotropic exponent  $\psi_{\alpha} = \psi = \frac{1}{2}$ . Equation (16) assumes that disorder enters in the exponential only via the Lyapunov exponent  $\gamma_D$ . While its presence is natural since the stretched exponential form requires a length scale, and thus the corresponding Lyapunov exponent of the underlying single-parameter scaling theory [49], it is not clear why  $A_{\alpha}$  and  $f_{\alpha}$  should be disorder independent. Nonetheless, as we show below, this hypothesis is compatible with our data. Finally, we mention that, unlike the mean correlations, the numerical prefactor  $c_{x,D}$  is the same for both even and odd separations  $r$ .

In Figs. 8(a) and (b) we plot respectively the transverse and longitudinal typical correlations for  $r = L/8 - 1$  and various chain sizes  $L$  and disorder strengths  $D$ . The insets (i) of those figures bring the raw data from which the SDRG prediction  $\ln|C_{\text{typ}}^{\alpha\alpha}| \sim -\sqrt{r}$  is confirmed.

We then replot the correlations as a function of  $(\gamma_D L)^{\psi}$  as shown in the insets (ii) of those figures. Apparently, the constant  $A_{\alpha}$  is disorder-independent. Moreover, the values of  $L$  used seem to be sufficiently large (at least for  $D \geq 0.4$ ) such that  $\chi_{\alpha,D} \approx 1$ . Therefore, it is safe to obtain the values of  $c_{\alpha,D}$  and  $A_{\alpha}$  by simply fitting Eq. (16) to our data.<sup>10</sup> The fitting values of  $c_{\alpha,D}$  and  $A_{\alpha} \sqrt{f_{\alpha}(1/8)}$  are plotted in Fig. 8(c). For  $D \leq 0.3$ , these are effective values [not in the asymptotic regime  $\gamma_D r \gg 1$ , as can be seen in insets (ii)]. The fitting values are consistent with  $A_{\alpha}$  and  $f_{\alpha}$  being disorder independent.

In order to proceed, as in the analysis of the mean correlation  $\overline{C^{xx}}$ , we need the relation between the numerical prefactor  $c_{\alpha,D}$  and the disorder strength  $D$ . Clearly, one needs a theory capable of capturing both the clean and the disorder critical behaviors. Here, however, we will simply try to connect the clean behavior  $C_{\text{clean}}^{\alpha\alpha} \sim c_{1,\alpha} r^{-\eta_{\alpha}}$  (with  $\eta_x = 1/2$  and  $\eta_z = 2$ )

<sup>10</sup> We consider only the data such that  $|C_{\text{typ}}^{xx}| < 2.5 \cdot 10^{-2}$  and  $|C_{\text{typ}}^{zz}| < 2.0 \cdot 10^{-4}$ . This is simply to ensure some meaning to the fitting function (16) when disorder is weak ( $D < 0.6$ ). As we explain latter on, this has no influence in our results.

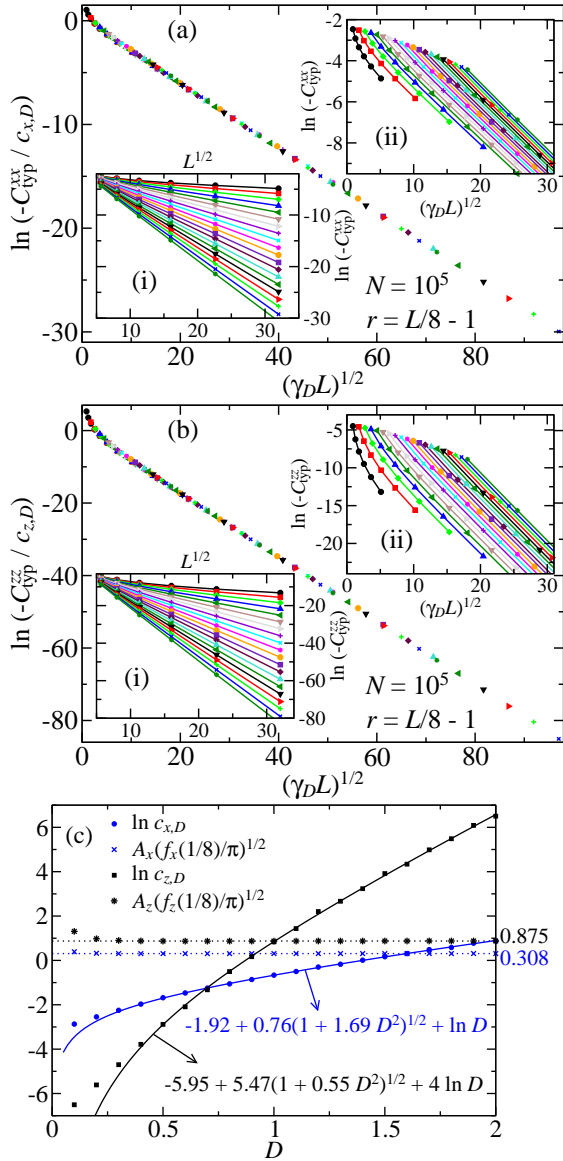


FIG. 8. Uncorrelated disorder model: the typical value of the (a) transverse and (b) longitudinal spin-spin correlations as a function of the system size  $L$  [inset (i)] and  $\gamma_D L$  [close up in inset (ii)], for various disorder strengths  $D$  and separation  $r = L/8 - 1$ . System sizes are  $L = 2^n$ , with  $n$  ranging from 5 to 10. Disorder strength varies from  $D = 0.1$  to 2.0 [topmost and bottommost curves in inset (i), respectively] in equal steps of 0.1. The lines are guide to the eyes. In panel (c),  $c_{\alpha,D}$  and  $A_\alpha$  are plotted against  $D$ . They are the best fits (16) to the data in insets (ii) (restricted to  $|C_{\text{typ}}^{\text{xx}}| < 2.5 \cdot 10^{-2}$  and  $|C_{\text{typ}}^{\text{zz}}| < 2.0 \cdot 10^{-4}$ ). The solid lines are the best fits to Eq. (17) restricted to  $D \geq 0.4$  and are used to obtain the data collapse in the main plots of panels (a) and (b).

to the strong-disorder one  $C_{\text{typ}}^{\alpha\alpha} \sim c_{\alpha,D} e^{-c_{2,\alpha} \sqrt{\gamma_D r}}$ . Assuming a sharp crossover at  $r = r_\alpha^* = c_{3,\alpha} \gamma_D^{-1}$ , continuity requires that  $\ln c_{\alpha,D} = p_\alpha + 2\phi_\alpha \ln D$ . However, this poorly fits the data in Fig. 8(c). We have tried several modifications of this scenario in order to improve the fit. They include adding one or two polynomials  $\propto D^n$  and power-laws  $\propto D^{-n}$ , and also changing

the prefactor of the logarithmic term. The worst modifications are those in which the logarithmic term is dropped out, implying that  $c_{\alpha,D} \propto D^{2\phi_\alpha}$  is very robust. The most successful modification is such that we admit a sharp crossover happening at  $r_\alpha^* = c_{3,\alpha} \gamma_D^{-1} + c_{4,\alpha}$ . The exponential in the typical correlation then acquires a dependence on  $D$  yielding to

$$\ln c_{\alpha,D} = o_\alpha + p_\alpha \sqrt{1 + q_\alpha D^2} + 2\phi_\alpha \ln D, \quad (17)$$

with  $o_\alpha$ ,  $p_\alpha$  and  $q_\alpha$  being fitting parameters. The fitting values are shown in Fig. 8(c) for which only the data for  $D \geq 0.4$  were used. The reason is that for smaller values of  $D$ , the slope  $A_\alpha$  is not fully saturated (due to the effects of the crossover function  $\chi_{\alpha,D}$ ). We have checked that changing any of the fitting parameters values by 5% does not change the quality of the fit, i.e., the reduced weighted error sum  $\bar{\chi}^2$  remains the same within the statistical error. This means that 5% is a reasonable estimate for the accuracy of our fit.

We now put Eq. (17) to test by assuming that it holds for all disorder strengths. In the main panels of Figs. 8(a) and (b), we plot  $C_{\text{typ}}^{\alpha\alpha}/c_{\alpha,D}$  as a function of  $\sqrt{\gamma_D L}$  (recall  $r/L \approx 1/8$  is fixed). Remarkably, and somewhat surprisingly, we obtain good data collapse even for the least disordered system studied  $D = 0.1$ . For small  $\sqrt{\gamma_D L}$ ,  $C_{\text{typ}}^{\alpha\alpha}/c_{\alpha,D}$  deviates from the pure stretched exponential, which is attributed to the crossover term  $\chi_{\alpha,D}(r)$ . The fact that the data collapse for all disorder strengths means that, to a good approximation, disorder enters in  $\chi_{\alpha,D}$  through the combination  $\gamma_D r$ , i.e.,  $\chi_{\alpha,D}(r) = \chi_\alpha(\gamma_D r)$ . Once more, this data collapse also supports that  $f_\alpha$  is a disorder-independent function.

We are now in the position to study the chord-length-correction function  $f_\alpha$  in Eq. (16). In Fig. 9, we plot  $C_{\text{typ}}^{\alpha\alpha}$  as a function of suitable combinations of  $r$ ,  $L$  and  $\gamma_D$ . For clarity, we show only a few data such as  $L = 2^n$ , with  $n = 7, 8$ , and 9, and  $D = 0.5, 1.0$ , and 2.0. As can be seen in the main panel of Fig. 9(a), the chord length  $\ell = \frac{L}{\pi} \sin(\pi r/L)$  is nearly enough for accounting all the finite-size effects. The combination  $\gamma_D \ell$  [see the inset of Fig. 9(b)] nearly collapses all the data. The role played by the crossover function  $\chi_{\alpha,D}$  and the chord-length-correction function  $f_{\alpha,D}$  are shown in the main panel of Fig. 9(b). We note that all curves converge to a single one in the large- $L$  limit, in agreement with the hypothesis (16). The dashed lines are the best fits restricted to the region  $\ell = \frac{L}{\pi} \sin(\frac{\pi r}{L}) > 0.5$  and considering only the large system size  $L = 512$ . The fitting values of  $A_\alpha$  and  $a_{2n,\alpha}$  are reported in Fig. 9(b). (Adding higher order terms do not improve our fit.) Notice the small correction to the chord length  $a_{2,4,\alpha} \ll 1$ , much smaller than those for the mean correlations. Interestingly, the crossover function  $\chi_{\alpha,D}$  is non-monotonic with respect to  $D$ . Notice that  $\chi_{\alpha,D}$  tends to 1 from above for weak disorder  $D \lesssim 1.0$ , and from below otherwise. Finally, we verified (not shown) that  $|\chi_{x,D} - 1|/|\chi_{z,D} - 1|$  is nearly a constant for large  $\gamma_D r$ .

We now turn our attention to the correlation function distribution. In the pioneering work by Fisher, it was conjectured that  $\ln |C^{\alpha\alpha}|/\sqrt{r}$  converges to a non-trivial distribution for large separation  $r$ . This conjecture was confirmed in Refs. 42 and 50 by numerically computing the distribution of  $\ln |C^{\alpha\alpha}|/\sqrt{r}$  for a fixed disorder strength  $D$ . We confirm this conjecture by studying the distribution of  $z =$



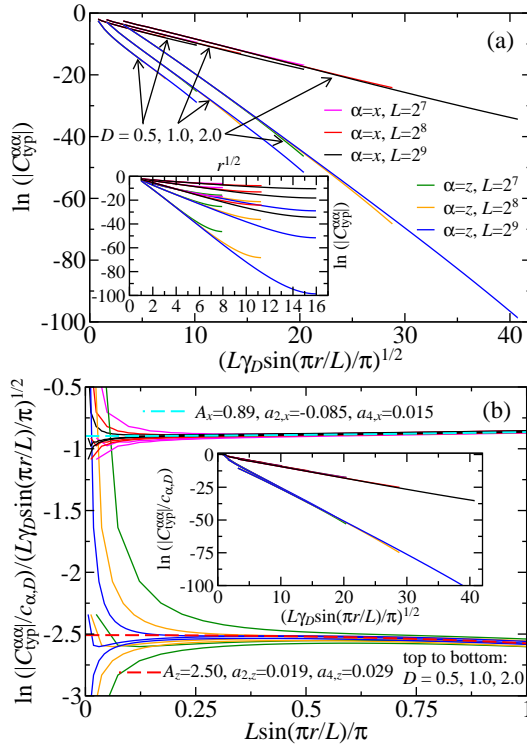


FIG. 9. The transverse and longitudinal typical value of the correlation function  $C_{\text{typ}}^{\alpha\alpha}(r)$  for chain sizes  $L = 2^n$ , with  $n = 7, 8$ , and  $9$ , and disorder strengths  $D = 0.5, 1.0$ , and  $D = 2.0$ . The corresponding legends are given in panel (a). The same data were plotted in different ways in the main panels and insets (see text). The dashed lines in panel (b) are the best fits according to Eq. (16).

$-\ln(|C^{\alpha\alpha}|/c_{\alpha,D})/A_{\alpha}\sqrt{\gamma_D L/\pi}$  for fixed separation  $r = L/2$  and disorder strength  $D = 1.0$ , for various system sizes  $L$ . As shown in Fig. 10(a) the distribution  $P_{\alpha}(z)$  converges to a non-trivial one for large  $L$ . According to Eq. (16), the first moment of  $P_x$  and  $P_z$  converges to the unity in the  $\gamma_D r \gg 1$  regime. We first notice that  $P_x$  and  $P_z$  are not equal. Also, both distributions are narrow. We have tried many different fitting functions. Since they are narrow, we tried Weibull and Gaussian distributions but with poor success. The most satisfactory one is

$$P_{\alpha}(z) = C_{\alpha} \exp\left(-\left|\frac{z}{\delta_{\alpha}} - \zeta_{\alpha}\right|^{\gamma_{\alpha}} + b_{\alpha}\left(\frac{\delta_{\alpha}}{z}\right)^{\gamma'_{\alpha}}\right), \quad (18)$$

where  $C_{\alpha}$  is a normalization constant, and  $\delta_{\alpha}$ ,  $\zeta_{\alpha}$ ,  $b_{\alpha}$ ,  $\gamma_{\alpha}$  and  $\gamma'_{\alpha}$  are fitting parameters with obvious interpretations. The first term in the exponential dictates the large-distance behavior  $\gamma_D r \gg 1$  which, naively, we expect to be near a Gaussian. Then,  $\gamma_{\alpha}$  is the corresponding exponent for the tail,  $\delta_{\alpha}$  would represent the width and  $\zeta_{\alpha}$  the rescaled offset. The second term dictates the low-distance behavior  $\gamma_D r \ll 1$  with corresponding exponent  $\gamma'_{\alpha}$ .<sup>11</sup> Notice that this term represents a

sharp cutoff for  $z < 0$ . We have tried to offset this term via  $z - z_0$  and found that  $|z_0| \lesssim 0.02$ . Surprisingly, our choice of  $z$  makes the  $P_{\alpha}(z < 0) = 0$ . Our fits extrapolated to  $L \rightarrow \infty$  are shown as solid lines in Fig. 10(a) and are numerically equal to  $\zeta_x = 0.65(5)$ ,  $\zeta_z = 1.1(2)$ ,  $\delta_x = 0.64(3)$ ,  $\delta_z = 0.62(2)$ ,  $\gamma_x = 1.71(3)$ ,  $\gamma_z = 2.11(5)$ ,  $b_x = 4.6(3)$ ,  $b_z = 8.7(5)$ ,  $\gamma'_x = 0.41(3)$ , and  $\gamma'_z = 0.19(2)$ .

We now step forward and study how  $P_{\alpha}$  depends on  $D$ . In Figs. 10(b) and (c) we plot the distribution of  $-\ln|C^{\alpha\alpha}|$  (shifted by its average and divided by its standard deviation) for various disorder strengths  $D$ , system sizes  $L$ , and separations  $r = L/8$  and  $L/2$ . For comparison, we replot the corresponding fits of panel (a) in panels (b) and (c), also shifted by the corresponding mean values (which are both equal to one)

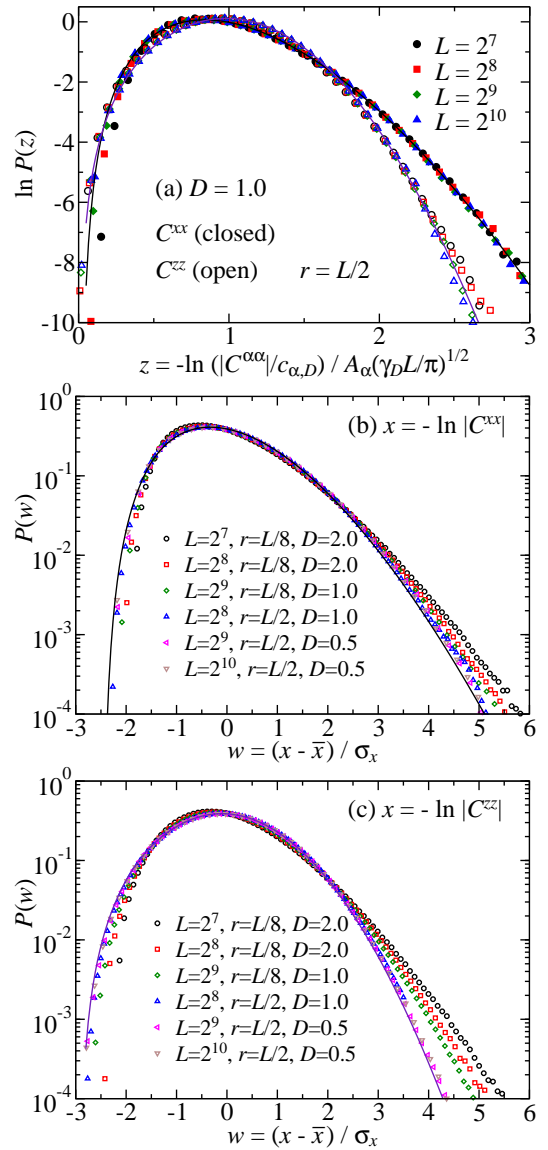


FIG. 10. Rescaled distribution of the correlation function  $C^{\alpha\alpha}(r)$ , for (a) fixed distance  $r = L/2$  and disorder strength  $D = 1.0$ , and (b) and (c) distances  $r = L/8$  and  $L/2$  and various disorder strengths  $D$  for various system sizes  $L$ . The lines are best fits of Eq. (18) (see text for details).

<sup>11</sup> We also have tried polynomials  $P_{\alpha} \propto z^{\lambda'_{\alpha}}$  and verified satisfactory fits with  $\lambda'_x \approx 5 \pm 1$  and  $\lambda'_z \approx 2.6 \pm 0.6$ .

and divided by the corresponding standard deviation (0.38 and 0.35, respectively for  $\alpha = x$  and  $\alpha = z$ ). For separations  $r = L/2$ , all distributions are clearly universal, i.e., disorder independent. For shorter separations  $r = L/8$ , the distributions differ from the universal one. Given the systematic tendency towards the universal distribution for larger and larger system sizes  $L$ , we then attribute this discrepancy to the fact that the limit of large separation has not been achieved for those cases. We therefore conclude that, in the large separation limit, the distribution of  $\ln|C^{\alpha\alpha}|/\sqrt{\gamma_D r}$  converges to a non-trivial, narrow and universal (disorder-independent) distribution.

#### IV. SPIN-SPIN CORRELATIONS FOR THE CORRELATED COUPLING CONSTANTS MODEL

In this section we report our results on the average and typical correlation functions for the case of correlated disorder in the model (1), which is defined by a set of coupling constants  $\{J_1, J_1, J_2, J_2, \dots, J_{L/2}, J_{L/2}\}$  (see Sec. II).

Unlike the uncorrelated disorder model, there is no analytical theory predicting the critical exponents. Here, our purpose is to determine them for the average and typical correlation functions.

In Fig. 11, we plot the typical correlations for various chain lengths  $L$  and disorder strengths  $D = 0.5$  and 1.0. Clearly, the

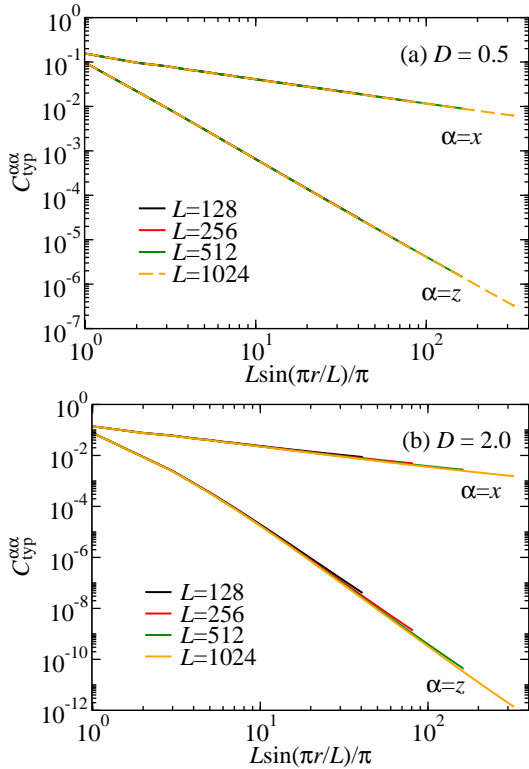


FIG. 11. The typical correlation functions as a function of the chord length (8) for the case of correlated disorder. The data were averaged over  $N = 10^5$  disorder realizations.

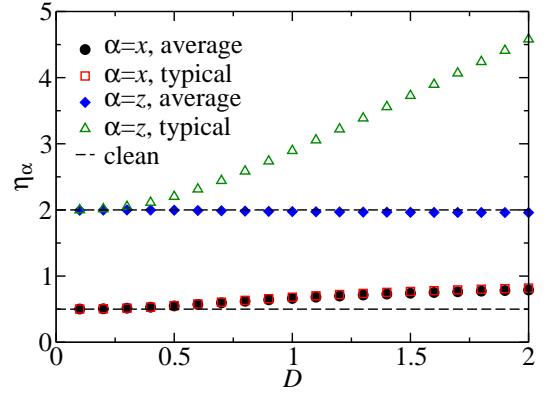


FIG. 12. The average and typical correlation function critical exponents  $\eta_{x,z}$  as a function of the disorder strength  $D$  for the correlated disorder model. The dashed lines correspond to the homogeneous (clean) system values.

chord length 8 is almost a perfect scaling variable.<sup>12</sup>

Clearly, the typical correlations decay algebraically, which is very distinct from their uncorrelated disorder counterpart. Evidently (not shown here), the average correlations also decays algebraically with the spin separation  $r$ . Simple fits restricted to the long-distance tail provide the corresponding exponents which are shown in Fig. 12.

For disorder strengths below the threshold  $D_c \approx 0.3$ , the exponent agrees with those of the clean system  $\eta_z = 4\eta_x = 2$ , as expected. Tuning the line of finite-disorder fixed points by increasing  $D$  beyond  $D_c$ , the exponents vary continuously and in a non-trivial fashion.

With respect to the transverse correlation, both typical and average exponents are equal within our statistical error, and increase monotonically but is bounded to 1. This suggests that the distribution of  $\ln|C^{xx}|$  has finite and small width for

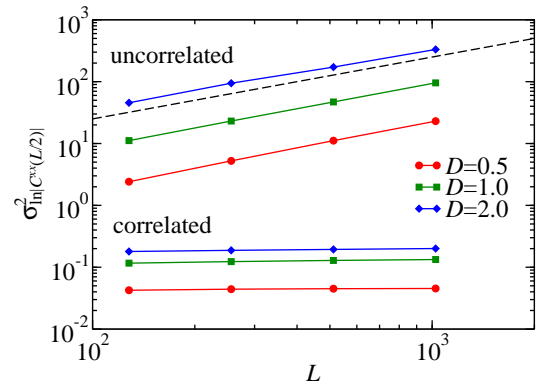


FIG. 13. The variance  $\sigma_x^2 = \overline{x^2} - \bar{x}^2$  of the transverse correlation  $x = \ln|C^{xx}(L/2)|$  as the chain size  $L$  is varied for different disorder strengths  $D$  for both the uncorrelated and correlated disorder models. The dashed line is the infinite-randomness prediction that  $\sigma_x^2 \sim L$ .

<sup>12</sup> Likewise, the chord length was verified to be nearly the correct scaling variable for the Rényi entanglement entropy for any disorder strength  $D$  [34].

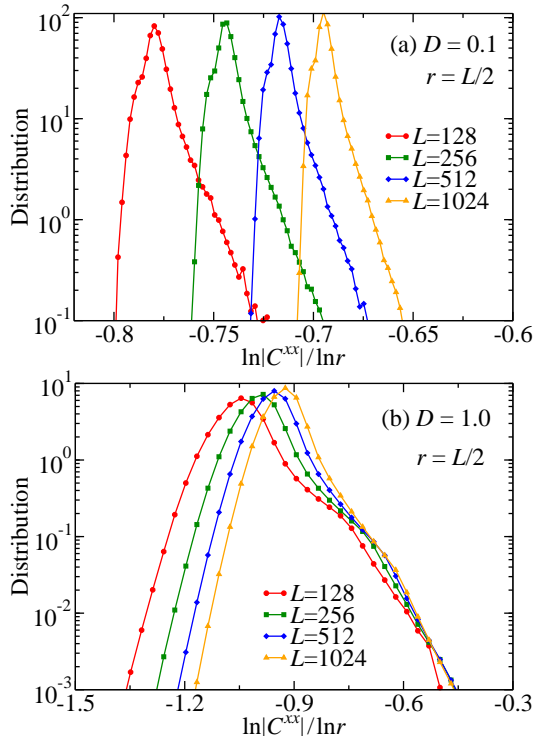


FIG. 14. Correlated disorder model: The distribution of the transverse correlation function  $C^{xx}(r)$  for disorder strengths (a)  $D = 0.1$  and (b)  $D = 1.0$  and  $r = L/2$ . The data was obtained from  $N = 10^3$  disorder realizations for panel (a) and  $N = 10^5$  for panel (b).

any distance  $r$  and system size  $L$  as can be verified in Figs. 13 and 14.

In contrast, the typical and average longitudinal correlations behave quite differently from each other. The average critical exponent remains equal to the clean one for all disorder strengths studied. The typical one increases linearly for  $D > D_c$  apparently without bounds. This implies that the width of the distribution of  $\ln|C^{zz}|/\ln r$  increases with  $D$ , as verified in Fig. 15, but is fixed for  $L$  and  $r$  (as we have verified but it is not shown here).

We end this section by calling attention to the striking difference between transverse and longitudinal correlations. Certainly, the ground state is far from the random singlet state of the uncorrelated disorder model. As pointed out in Ref. 34, the entanglement properties of the correlated disorder model shares many similarities with the clean ground state. The fact that typical and average longitudinal correlations are quite different points towards less similarities.

## V. CONCLUSIONS

In this work we have studied the spin-spin correlation functions for the quantum critical spin-1/2 XX chain in the case of uncorrelated and correlated coupling constants (see Sec. II). In the former case, the chain is governed by a universal (disorder independent) infinite-randomness fixed point, while in the latter, it is governed by the clean fixed point for weak disorder ( $D < D_c$ ) and by a line of finite-randomness fixed points

tuned by the disorder strength ( $D > D_c$ ).

For uncorrelated disorder, we have proposed and numerically verified that the correlations in Eqs. (7), (10), (16) are good approximations in the regime  $\gamma_D r \gg 1$  (not restricted to the thermodynamic limit  $r \ll L$ ) for periodic boundary conditions. We have shown that the chord length (8) is not the true scaling variable, exhibiting small corrections for the mean correlations and even smaller for the typical ones. We have parameterized and quantified these corrections through the function  $f_\alpha$  in Eq. (9). In principle, these corrections should be non-universal, i.e., disorder dependent. While this may be indeed the case, we could fit our data using the hypothesis that  $f_\alpha$  is universal. Naturally, deciding whether  $f_\alpha$  is universal or not requires better statistics and larger systems which are out of our current reach.

In addition, we have studied the corresponding non-universal numerical prefactors and linked them to the corresponding Lyapunov exponent (12) which, ultimately, link them to the disorder strength. Surprisingly, we have determined an accurate scaling as quantified in Eqs. (14) and (17) for the mean transverse correlations and the typical longitudinal and transverse correlations, respectively. In general, these prefactors and their scaling with a crossover length depend on the dimensions of the related relevant and irrelevant operators. It is not the scope of the present work to find those operators and their dimensions. We leave this as an open question and hope that our findings serve as future motivation.

We have also studied the distribution of correlations. We have confirmed (not for the first time) the conjecture that the quantity  $\ln|C^{\alpha\alpha}|/\sqrt{r}$  converges to a non-trivial distribution in

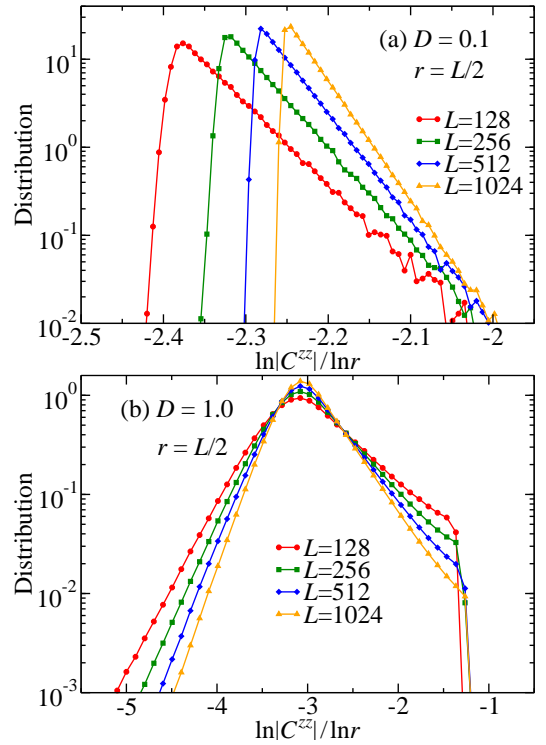


FIG. 15. Same as Fig. 14, but for the longitudinal component of the correlation function.

the large-separation regime. In addition, based on the knowledge built from the typical correlation and its relation with the Lyapunov exponent, we have numerically determined that, in the large separation limit, the distribution of  $\ln|C^{\alpha\alpha}|/\sqrt{\gamma_D r}$  converges to a non-trivial  $\alpha$ -dependent, narrow and universal (disorder-independent) distribution quantified in Eq. (18).

It is desirable to generalize our results to other anisotropies  $\Delta \neq 0$ . It is not entirely clear whether a single-parameter scaling will be possible for all  $-\frac{1}{2} < \Delta \leq 1$ . Assuming that the SDRG method is indeed asymptotically exact in this range of anisotropies, it is then plausible that our results generalize (since  $\Delta \rightarrow 0$  under the SDRG flow) at the simple cost of correcting the Lyapunov exponent. Based on the field-theory methods of Ref. 9 and 25, it is plausible that Eq. (12) generalizes to  $\gamma_D \sim D^{\frac{2}{3-2K}}$ , with the Luttinger parameter  $K = 1 - \pi^{-1} \arccos(\Delta)$ . Evidently, the values of non-universal quantities such as  $a_{2n,\alpha}$  in (9) may depend on  $\Delta$ .

Last but not least, we have shown the importance of the finite-size effect and numerical instabilities when characterizing the random-singlet state. They are so strong that can mimic logarithmic corrections to the correct scaling (see Fig. 6).

Conversely, for the correlated disorder model we have shown that the typical correlation functions decay as a power law (see Fig. 11), just like the mean correlations. The corre-

sponding exponents were determined (see Fig. 12) and vary continuously for  $D > D_c \approx 0.3$ . While the exponents for the mean and typical transverse correlations remain nearly equal (implying a narrow distribution of correlations), the behavior is strikingly different for the longitudinal correlations, a consequence of the fact that the distribution of longitudinal correlations are much broader. In addition, we have determined the chord length is not the correct scaling variable (but it is a very good approximation to it). The fact that the transverse and longitudinal correlations behave so differently implies that the random-singlet state is far from being a good approximation of the true ground state even when  $D \rightarrow \infty$ . The infinite-randomness low-energy physics of the uncorrelated disorder model is not adiabatically connected to the strong but finite-randomness behavior of the correlated disorder model.

## ACKNOWLEDGMENTS

We would like to thank Anders Sandvik and Róbert Juhász for useful discussions, and Nicolas Laflorencie for bringing Ref. 14 to our attention. This study was financed in part by the Coordenação de Aperfeiçoamento de Pessoal de Nível Superior - Brasil (CAPES) - Finance Code 001, and also by the Brazilian funding agencies CNPq and FAPESP.

All authors contributed equally to this work.

- 
- [1] S. K. Ma, C. Dasgupta, and C. H. Hu, *Phys. Rev. Lett.* **43**, 1434 (1979).
- [2] C. Dasgupta and S. K. Ma, *Phys. Rev. B* **22**, 1305 (1980).
- [3] R. N. Bhatt and P. A. Lee, *Phys. Rev. Lett.* **48**, 344 (1982).
- [4] F. Iglói and C. Monthus, *Phys. Rep.* **412**, 277 (2005).
- [5] F. Iglói and C. Monthus, *The European Physical Journal B* **91**, 290 (2018).
- [6] D. S. Fisher, *Phys. Rev. Lett.* **69**, 534 (1992).
- [7] D. S. Fisher, *Phys. Rev. B* **50**, 3799 (1994).
- [8] T. Vojta, *J. Phys. A: Math. Gen.* **39**, R143 (2006).
- [9] C. A. Doty and D. S. Fisher, *Phys. Rev. B* **45**, 2167 (1992).
- [10] N. Laflorencie, H. Rieger, A. Sandvik, and P. Henelius, *Phys. Rev. B* **70**, 054430 (2004).
- [11] J. A. Hoyos and G. Rigolin, *Phys. Rev. A* **74**, 062324 (2006).
- [12] J. A. Hoyos, A. P. Vieira, N. Laflorencie, and E. Miranda, *Phys. Rev. B* **76**, 174425 (2007).
- [13] Z. Ristivojevic, A. Petković, and T. Giamarchi, *Nucl. Phys. B* **864**, 317 (2012).
- [14] Y. R. Shu, D. X. Yao, C. W. Ke, Y. C. Lin, and A. W. Sandvik, *Phys. Rev. B* **94**, 1 (2016).
- [15] J. C. Getelina, T. R. de Oliveira, and J. A. Hoyos, *Physics Letters A* **382**, 2799 (2018).
- [16] Y.-R. Shu, M. Dupont, D.-X. Yao, S. Capponi, and A. W. Sandvik, *Phys. Rev. B* **97**, 104424 (2018).
- [17] G. Theodorou, *Phys. Rev. B* **16**, 2264 (1977).
- [18] T. Masuda, A. Zheludev, K. Uchinokura, J.-H. Chung, and S. Park, *Physical Review Letters* **93**, 077206 (2004).
- [19] T. Shiroka, F. Casola, W. Lorenz, K. Prša, A. Zheludev, H.-R. Ott, and J. Mesot, *Phys. Rev. B* **88**, 054422 (2013).
- [20] T. Shiroka, F. Eggenschwiler, H.-R. Ott, and J. Mesot, *Phys. Rev. B* **99**, 035116 (2019).
- [21] E. Lieb, T. Schultz, and D. Mattis, *Ann. Phys.* **16**, 407 (1961).
- [22] B. M. McCoy, *Phys. Rev.* **173**, 531 (1968).
- [23] A. Luther and I. Peschel, *Phys. Rev. B* **12**, 3908 (1975).
- [24] F. D. M. Haldane, *Phys. Rev. Lett.* **45**, 1358 (1980).
- [25] T. Giamarchi and H. J. Schulz, *Phys. Rev. B* **39**, 4620 (1989).
- [26] R. R. P. Singh, M. E. Fisher, and R. Shankar, *Phys. Rev. B* **39**, 2562 (1989).
- [27] K. A. Hallberg, P. Horsch, and G. Martínez, *Phys. Rev. B* **52**, R719 (1995).
- [28] S. Lukyanov and A. Zamolodchikov, *Nucl. Phys. B* **493**, 571 (1997).
- [29] I. Affleck, *Journal of Physics A: Mathematical and General* **31**, 4573 (1998).
- [30] S. Lukyanov, *Nuclear Physics B* **522**, 533 (1998).
- [31] T. Hikihara and A. Furusaki, *Phys. Rev. B* **58**, R583 (1998).
- [32] S. Lukyanov, *Phys. Rev. B* **59**, 11163 (1999).
- [33] J. A. Hoyos, N. Laflorencie, A. P. Vieira, and T. Vojta, *EPL Europhysics Lett.* **93**, 30004 (2011).
- [34] J. C. Getelina, F. C. Alcaraz, and J. A. Hoyos, *Phys. Rev. B* **93**, 045136 (2016).
- [35] A. Macdiarmid, J. Chiang, A. Richter, and A. Epstein, *Synthetic Metals* **18**, 285 (1987).
- [36] D. H. Dunlap, H.-L. Wu, and P. W. Phillips, *Phys. Rev. Lett.* **65**, 88 (1990).
- [37] H.-L. Wu and P. Phillips, *Phys. Rev. Lett.* **66**, 1366 (1991).
- [38] V. L. Quito, J. A. Hoyos, and E. Miranda, *Phys. Rev. Lett.* **115**, 167201 (2015).
- [39] V. L. Quito, P. L. S. Lopes, J. A. Hoyos, and E. Miranda, *Eur. Phys. J. B* **93**, 17 (2020).
- [40] V. L. Quito, P. L. S. Lopes, J. A. Hoyos, and E. Miranda, *Phys. Rev. B* **100**, 224407 (2019).
- [41] K. Hamacher, J. Stolze, and W. Wenzel, *Phys. Rev. Lett.* **89**, 127202 (2002).



- [42] P. Henelius and S. M. Girvin, [Phys. Rev. B \*\*57\*\*, 11457 \(1998\)](#).
- [43] F. Iglói, R. Juhász, and H. Rieger, [Phys. Rev. B \*\*61\*\*, 552 \(2000\)](#).
- [44] J. C. Xavier, J. A. Hoyos, and E. Miranda, [Phys. Rev. B \*\*98\*\*, 195115 \(2018\)](#).
- [45] H. Rieger and F. Iglói, [Phys. Rev. Lett. \*\*83\*\*, 3741 \(1999\)](#).
- [46] A. K. Ibrahim, H. Barghathi, and T. Vojta, [Phys. Rev. E \*\*90\*\*, 042132 \(2014\)](#).
- [47] I. Affleck, D. Gepner, H. J. Schulz, and T. Ziman, [J. Phys. \*\*A22\*\*, 511 \(1989\)](#).
- [48] M. Fagotti, P. Calabrese, and J. E. Moore, [Phys. Rev. B \*\*83\*\*, 1 \(2011\)](#).
- [49] H. Javan Mard, J. A. Hoyos, E. Miranda, and V. Dobrosavljević, [Phys. Rev. B \*\*90\*\*, 125141 \(2014\)](#).
- [50] A. Young and H. Rieger, [Phys. Rev. B \*\*53\*\*, 8486 \(1996\)](#).